

Ultrasonic Behavior near the Spin-Flop Transitions of Hematite

Y. SHAPIRA

Francis Bitter National Magnet Laboratory, Massachusetts Institute of Technology,
Cambridge, Massachusetts 02139*

*and
Physics Department and Laboratory for Research on the Structure of Matter,†
University of Pennsylvania, Philadelphia, Pennsylvania 19104*

(Received 14 February 1969)

Ultrasonic propagation in natural single crystals of hematite (α -Fe₂O₃) was studied in magnetic fields up to 200 kG at various temperatures between 4.2 and 300°K. Anomalies in the ultrasonic attenuation were observed near: (1) the spin-flop transition at H_{c11} (in a field parallel to the trigonal axis), (2) the spin-flop transition at H_{c1} (in a field normal to the trigonal axis), and (3) the Morin transition. Anomalies in the velocity of some acoustical modes of propagation were also observed at H_{c11} . The temperature variation of H_{c11} and H_{c1} was studied in one of the hematite crystals which had a low impurity content. At 77°K, $H_{c11}=68.2 \pm 0.7$ kG and $H_{c1}=160.8 \pm 2$ kG. The Morin transition in this crystal occurs at $T_M=(260.6 \pm 0.5)$ °K. The ultrasonic data can be accounted for by considering the motion of domain walls under the action of an oscillating elastic stress. Other explanations are also considered. The data for H_{c11} and H_{c1} are compared with the results of other workers.

I. INTRODUCTION

RECENTLY there has been a great deal of interest in ultrasonic attenuation near magnetic phase transitions. This interest has centered mainly on the critical attenuation near the Curie point of ferromagnets (Néel point for antiferromagnets), which is studied in zero magnetic field.¹ In addition, there has been interest in the ultrasonic behavior near magnetic phase transitions which occur in a magnetic field. In a previous paper² it was shown that striking effects in the ultrasonic attenuation occur near the spin-flop transition of the simple uniaxial antiferromagnet MnF₂. The present work is a natural extension of the work described in Ref. 2 to a more complicated antiferromagnetic material.

Hematite (α -Fe₂O₃) is a substance which is essentially antiferromagnetic below the Néel temperature, $T_N \approx 960$ °K. In zero magnetic field hematite undergoes a phase transition at $T_M \approx 260$ °K, known as the Morin transition,^{3,4} where the orientation of the spins relative to the rhombohedral (trigonal) lattice changes. At $T_N > T > T_M$ the spins lie in the trigonal plane and are slightly canted relative to each other.^{5,6} The canting of the spins leads to a weak net ferromagnetic moment (Dzyaloshinsky moment) in the trigonal plane. At $T < T_M$, the spins are directed along or close to the trigonal axis. It is possible to flip the direction of the spins, at $T < T_M$, from the trigonal axis to the trigonal plane by applying a sufficiently strong magnetic field. For a magnetic field \mathbf{H} applied along the trigonal axis

the spin-flop transition is a first-order transition accompanied by a discontinuous change in the magnetization at the transition field H_{c11} . Several investigators⁷⁻¹² have found that H_{c11} is in the range 63–68 kG at 77°K. There have also been several studies of the reorientation of the spins in a magnetic field applied normal to the trigonal axis.^{9,11-15} The available data indicate that for this field orientation the transition field H_{c1} at 77°K is in the range 130–145 kG (our own value is somewhat higher).

This paper is devoted to ultrasonic studies near the magnetic phase transitions at H_{c11} , H_{c1} , and T_M . Internal friction near T_M has been previously investigated by Makkay *et al.*¹⁶ Because large synthetic single crystals of hematite could not be obtained, the present work was carried out on natural crystals from Elba and Brazil. Most of the work concentrated on one sample from Brazil which had a low impurity content, and which exhibited sharp magnetic phase transitions.

This paper is arranged as follows. In Sec. II a dis-

¹ S. Foner, in *Proceedings of The International Conference on Magnetism, Nottingham, 1964* (The Institute of Physics and The Physical Society, London, 1964), p. 438.

² N. Blum, A. J. Freeman, J. W. Shaner, and L. Grodzins, *J. Appl. Phys.* **36**, 1169 (1965).

³ T. Kaneko and S. Abe, *J. Phys. Soc. Japan* **20**, 11 (1965); **21**, 451 (1966).

⁴ P. J. Besser, A. H. Morrish, and C. W. Searle, *Phys. Rev.* **153**, 632 (1967).

⁵ V. I. Ozhogin and V. G. Shapiro, *Zh. Eksperim. i Teor. Fiz. Pis'ma v Redaktsiyu* **6**, 467 (1967) [English transl.: *Soviet Phys.—JETP Letters* **6**, 7 (1967)]; *Zh. Eksperim. i Teor. Fiz.* **54**, 96 (1968) [English transl.: *Soviet Phys.—JETP* **27**, 54 (1968)].

⁶ R. A. Voskanyan, R. Z. Levitin, and V. A. Shchurov, *Zh. Eksperim. i Teor. Fiz.* **53**, 459 (1967); **54**, 790 (1968) [English transl.: *Soviet Phys.—JETP* **26**, 302 (1968); **27**, 423 (1968)].

⁷ J. Kaczér and T. Shalnikova, in *Proceedings of The International Conference on Magnetism, Nottingham, 1964* (The Institute of Physics and The Physical Society, London, 1964), p. 589.

⁸ P. J. Flanders and S. Shtrikman, *Solid State Commun.* **3**, 285 (1965); G. Cinader, P. J. Flanders, and S. Shtrikman, *Phys. Rev.* **162**, 419 (1967).

⁹ P. J. Flanders, *J. Appl. Phys.* **40**, 1247 (1969).

¹⁰ R. W. Makkay, G. H. Geiger, and M. E. Fine, *J. Appl. Phys.* **33**, 914 (1962).

* Supported by the U. S. Air Force Office of Scientific Research.
† Work supported in part by the U. S. Advanced Research Project Agency.

¹ B. Luthi and R. J. Pollina, *Phys. Rev.* **167**, 488 (1968).

² Y. Shapira and J. Zak, *Phys. Rev.* **170**, 503 (1968). See also Y. Shapira, *Phys. Letters* **24A**, 361 (1967).

³ F. J. Morin, *Phys. Rev.* **78**, 819 (1950).

⁴ C. G. Shull, W. Strauser, and E. O. Wollan, *Phys. Rev.* **83**, 333 (1951).

⁵ I. Dzyaloshinsky, *J. Phys. Chem. Solids* **4**, 241 (1958).

⁶ T. Moriya, *Phys. Rev.* **120**, 91 (1960).

discussion of the experimental techniques and of the natural hematite crystals is given. The results of ultrasonic attenuation and velocity measurements near H_{c11} and H_{c1} , as well as the temperature dependence of H_{c11} and H_{c1} , are presented in Sec. III. Several mechanisms which may be responsible for the observed ultrasonic behavior, and also the temperature variation of H_{c11} and H_{c1} , are discussed in Sec. IV.

II. EXPERIMENTAL PROCEDURE

Ultrasonic measurements were carried out on several natural single crystals of hematite in the temperature range $4.2^\circ\text{K} \leq T \leq 300^\circ\text{K}$. Longitudinal and shear ultrasonic pulses of 0.5–2- μsec duration were generated and received with *X*-cut and *Y*-cut quartz transducers, respectively. Frequencies from 7.5 to 60 MHz were obtained by operating at the fundamental frequency of the transducers (8 to 12 MHz) or in one of the overtones. A single transducer was used in each case for both generating and receiving the signals. Acoustical bonds between the transducer and the sample were made either with Dow Corning 200 silicone fluid having a viscosity of 30 000 cs at 25°C , or with Nonaq stopcock grease. The former was found to be preferable at $T \lesssim 200^\circ\text{K}$, whereas better results were obtained with the latter at $T \gtrsim 200^\circ\text{K}$.

The variation of the ultrasonic attenuation with external magnetic field H , or temperature T , was measured by gating one of the acoustical echoes, integrating it, and recording the output as a function of H or T . In general, this procedure is not entirely reliable, since the coupling between the transducer and the sample may change with T , and possibly with H . Such a change in the coupling would lead to a variation in the height of the acoustical echoes even if the attenuation in the sample remains constant. To safeguard against this difficulty, the essential features of the attenuation data obtained by the technique described above were checked by measuring the difference in the heights of successive acoustical echoes as a function of H or T . While the latter procedure is reliable, it is tedious, since the measurements are carried out point by point. All the data which are presented below were obtained using the first procedure which employs continuous recording, but the essential features in each case were verified using the second procedure.

Some care had to be exercised with shear waves. For shear waves propagating along the trigonal axis, an internal conical refraction should occur.^{17,18} If the dimension of the sample along the trigonal direction is large compared to the dimensions perpendicular to it, then the sound beam may hit the side walls. For this reason the length along the trigonal axis was shortened in some cases, which resulted in an improvement of the

quality of the echo patterns. Also, for propagation along a binary axis, there exist two nondegenerate shear modes. In general, both modes will be generated simultaneously by a shear transducer unless it is polarized along special directions in the binary plane. To obtain reproducible and clear cut results it was necessary to vary the polarization of the *Y*-cut transducer in the binary plane until only one of the two shear modes was present. The same was true for shear waves propagating along a bisectrix direction.

Two types of ultrasonic velocity measurements were performed. One type involved the variation of the phase velocity with H , which was measured using a technique which has been described earlier.¹⁹ Changes of a few parts in 10^4 in the phase velocity could be detected easily. The second type of velocity measurement was carried out by observing the video signal (i.e., signal proportional to the amplitude of the rf signal) of the echo pattern on an oscilloscope and noting any change in the time-separation between the echoes as H was varied. The time separation between echoes was taken to be the time between the maximum video signal of one echo and the maximum video signal of a successive echo. Velocity changes greater than 1% could be measured in this fashion. It is important to note that when strong ultrasonic absorption is present, the velocity measured by the second technique is not necessarily equal to the phase velocity which is measured by the first technique.²⁰

Measurements at 4.2 and 77°K were performed in liquid helium and liquid nitrogen, respectively. The magnetic field variation of the attenuation in the temperature interval $77^\circ\text{K} \leq T \leq 270^\circ\text{K}$ was measured in the following way: The sample was mounted on a copper block and was placed in a Dewar filled with liquid nitrogen. The liquid nitrogen was then blown off and the sample was allowed to drift slowly to room temperature. Typically, it took a few hours for the sample to warm from 77 to 270°K . Measurements were taken "on the fly." The temperature was measured with a platinum thermometer embedded in the copper block on which the sample was mounted.

The temperature variation of the attenuation near T_M , in zero or low magnetic field, was measured as follows: The sample was mounted on a copper block and the whole arrangement was surrounded by a copper can and was inserted into Freon-11 (trichlorofluoromethane). The temperature was varied by pumping on the Freon-11, and was measured with a platinum thermometer as described earlier.

High dc magnetic fields up to 200 kG were generated in Bitter-type solenoids. The magnetic field in these magnets was known to an accuracy of 1%.

Five samples which were prepared from natural hematite crystals were used in the present work. Four of the samples came from Elba and one came from Brazil.

¹⁷ S. Epstein and A. P. deBretteville, Jr., Phys. Rev. **138**, A771 (1965).

¹⁸ Y. Eckstein, A. W. Lawson, and D. H. Reneker, J. Appl. Phys. **31**, 1534 (1960).

¹⁹ L. J. Neuringer and Y. Shapira, Phys. Rev. **148**, 231 (1966).

²⁰ L. Brillouin, *Wave Propagation and Group Velocity* (Academic Press Inc., New York, 1960).

The samples Elba-1 and Elba-2 were obtained from Professor D. R. Wones of MIT Geology Department. Samples Elba-3 and Elba-4 were cut from one large ($5 \times 3.5 \times 1.5$ cm, approx) single crystal obtained from Professor C. Frondel of Harvard Geology Department. The sample Brazil-1 was cut from a mineral obtained from Ward's Natural Science Establishment, Inc., Rochester, N. Y. The fabricated samples were rectangular in shape with faces normal, within 0.5° , to a binary, a bisectrix and the trigonal directions. Opposite faces of each sample were parallel and flat and were hand-lapped for ultrasonic work. The separation between parallel faces varied from 4 to 11 mm.

The most extensive data were taken on the sample Brazil-1. This sample, with dimensions of about $5 \times 5 \times 10$ mm, contained three thin (0.05 to 0.15 mm thick) twin lamellae, which were all parallel to each other. The lamellae were parallel to the (10 $\bar{1}$ 1) plane [in reference to the morphological unit cell, or (10 $\bar{1}$ 2) plane in reference to the structural unit cell] which makes an angle of $57^\circ 36'$ with the trigonal plane.^{21,22} The crystallographic orientation of these lamellae can be obtained from the orientation of the bulk of the sample by rotating about an axis normal to the (10 $\bar{1}$ 1) plane by 180° .²¹ While the volume occupied by the twin lamellae was small compared to the total volume of the sample, the magnetic transitions of the lamellae did give rise to weak but observable ultrasonic effects (see Ref. 24). Semi-quantitative spectroscopic analysis of a sample obtained from the same natural crystal from which the sample Brazil-1 was cut gave the following concentrations, in ppm, for the principal impurities: Al, from 10 to 100; Mn \sim 10; Mg \sim 10; Ti \sim 10; Sn \sim 10; Si, from 1 to 10; Ga, from 1 to 10; Cu \sim 1.

III. EXPERIMENTAL RESULTS

The experimental results are presented in two sections. Section III A is devoted to the spin-flop transition with \mathbf{H} parallel (or nearly parallel) to the trigonal axis. Most of this section is taken up by attenuation data for many acoustical modes of propagation near the spin-flop transition at 77 and 4.2°K. Some measurements of the change in the ultrasonic velocity at these two temperatures are also reported. Section III A concludes with the temperature variation of H_{c11} . Section III B is devoted to the magnetic phase transition with \mathbf{H} normal to the trigonal axis. Since the phase transition at H_{c1} had not been as thoroughly investigated in the past as the one at H_{c11} , the temperature dependence of the transition field H_{c1} was studied in detail. The observation of the Morin transition, at $H=0$, by ultrasonic means is also included (somewhat arbitrarily) in Sec. III B.

Of the five samples used in the present work, the results obtained in the sample from Brazil were the

most striking in two respects. First, the magnetic phase transitions in this sample were much sharper than in the other four samples. Second, the magnitudes of the attenuation changes near the phase transitions of Brazil-1 were comparable to or larger than those observed in the four Elba samples. For this reason, the results which are presented below are, for the most part, results which were obtained in Brazil-1. *Unless otherwise specified it will be understood that we refer to the sample Brazil-1.*

A. Field Parallel to Trigonal Axis

The magnetic field variation of the attenuation of longitudinal and shear ultrasonic waves propagating along the binary, bisectrix, and trigonal directions was measured at 77°K in magnetic fields up to 100 kG. Some attenuation measurements were also carried out at 4.2°K and at $77^\circ\text{K} < T < 300^\circ\text{K}$. In addition, the variation of the ultrasonic velocity with H was measured in a few selected cases. The ultrasonic velocities of the various acoustical modes which were excited in these experiments are listed in Table I. Each mode is characterized by the direction of its propagation vector \mathbf{q} and the direction of ion displacement ξ . The accuracy of these velocity measurements was better than 2%. Equations relating the velocities of the various modes to the elastic constants can be found in Refs. 17 and 18.

A detailed account of the experimental results at H_{c11} will be given separately for each mode of propagation. Since these accounts are, however, somewhat lengthy, it is useful to describe at the outset some of the salient features of the data.

In general, for a given acoustical mode the attenuation exhibited a sharp peak at H_{c11} (see, for example, Fig. 1) and/or rose sharply at H_{c11} and remained high at $H > H_{c11}$ (see, for example, Fig. 2). These two features will be called "attenuation peak" and "attenuation edge," respectively. The attenuation edge disappeared as \mathbf{H} was tilted away from the trigonal axis, but the attenuation peak remained although it moved to a higher field. The behavior of the attenuation of each mode at H_{c11} for $T=77^\circ\text{K}$ is characterized succinctly in the last column of Table I. A more complete account of

TABLE I. The velocity of sound V (at 77°K and $H=0$), and the characteristic behavior of the attenuation at H_{c11} ($T=77^\circ\text{K}$), for several modes of propagation. The binary, bisectrix, and trigonal directions are labeled as x , y , and z , respectively.

\mathbf{q}	ξ	Type of mode	V (10^5 cm/sec)	Behavior at H_{c11} ($T=77^\circ\text{K}$)
x	x	longitudinal	8.3	peak and edge
x	\dots	fast shear	4.55	edge
x	\dots	slow shear	3.87	edge
y	y	longitudinal	8.3	peak and edge
y	x	shear	4.31	edge
y	z	shear	4.13	edge
z	z	longitudinal	7.8	peak
z	normal to z	shear	4.18	edge

²¹ Anthony N. Mariano (private communication).

²² Dana's System of Mineralogy (John Wiley & Sons, Inc., New York, 1963), 7th ed., Vol. I.

the attenuation data and the results of velocity measurements are given below. In this discussion the *binary*, *bisectrix*, and *trigonal* directions are labeled as x , y , and z , respectively.

1. $q \parallel \xi \parallel z$ —Longitudinal Wave, $T=77, 4.2^\circ K$

Attenuation measurements were carried out with 10–50-MHz waves at $77^\circ K$. With $\mathbf{H} \parallel z$, a sharp attenuation peak occurred at 68.2 ± 0.7 kG. This field is in good agreement with the value of H_{c11} obtained from magnetization measurements in pulsed fields performed by Foner on the same sample,²³ and is also in agreement with earlier work.^{7–12} The full width at half-height of the attenuation peak was ~ 200 G. The height of the peak varied somewhat from run to run but was about 1–2 dB/cm at 30 MHz and approximately the same at 50 MHz. A typical recorder tracing of the attenuation peak at H_{c11} is shown in Fig. 1.

The dependence of the attenuation peak on the angle θ between \mathbf{H} and the z axis was measured at $77^\circ K$ with a 30-MHz wave and for $0^\circ < \theta < 24^\circ$. As θ increased, the attenuation peak was reduced in height, became broader, and its center moved to a higher magnetic field. At $\theta = 24^\circ$ the attenuation peak was several kG wide and its center was about 20 kG higher than at $\theta = 0$.

Some measurements of the phase velocity of a 30-MHz wave were made at $77^\circ K$ with $\mathbf{H} \parallel z$. A sharp dip of about 0.07% in the phase velocity was observed at H_{c11} .

Two runs with 30-MHz waves were performed at $4.2^\circ K$. In one run a small sharp attenuation peak was observed at H_{c11} , but the peak was not observed in the second run.

Attenuation measurements on the samples Elba-1, 2, and 3, performed at $77^\circ K$, showed no noticeable effect near H_{c11} .

2. $q \parallel z, \xi$ in xy Plane—Shear Wave, $T=77^\circ K$

Attenuation measurements with 8–30-MHz waves and with $\mathbf{H} \parallel z$ showed that a large attenuation edge exists at H_{c11} . The magnitude of the attenuation edge was greater than 10 dB/cm at 13 and 30 MHz, so that no acoustical echoes could be detected at $H > H_{c11}$. Figure 2 shows a recorder tracing of the attenuation edge at H_{c11} .

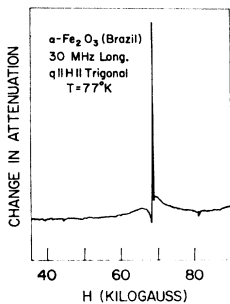


FIG. 1. Recorder tracing of the attenuation of a 30-MHz longitudinal wave with $q \parallel \mathbf{H} \parallel z$.

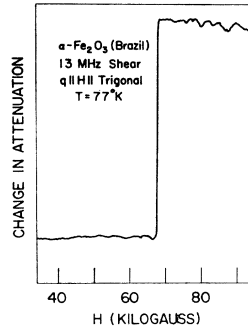


FIG. 2. Recorder tracing of the attenuation of a 13-MHz shear wave with $q \parallel \mathbf{H} \parallel z$. The recorder response to the attenuation is non-linear. The essentially flat part of the curve at $H > H_{c11}$ corresponds to the absence of detectable echoes.

When the magnetic field made an angle $\theta \approx 3^\circ$ with the z axis, the attenuation increased abruptly near H_{c11} , but then decreased monotonically with increasing magnetic field. The attenuation at fields well above H_{c11} was smaller than in the case $\theta = 0$, and it was possible to observe several acoustical echoes.

Attenuation measurements at $77^\circ K$ and with $\mathbf{H} \parallel z$ were also carried out on the samples Elba-1, 3, and 4. With 10–50-MHz waves, a large attenuation edge was observed in the range 62–70 kG. This attenuation edge was several kG wide. At the higher frequencies, the attenuation edge was preceded by a slow monotonic increase in the attenuation.

3. $q \parallel \xi \parallel x$ —Longitudinal Wave, $T=77, 4.2^\circ K$

Attenuation measurements were carried out at $77^\circ K$ with 10–60-MHz waves. When \mathbf{H} was as close as possible to the z axis, an attenuation edge, similar to the one shown in Fig. 2, was observed. The magnitude of this edge was greater than 5 dB/cm at 60 MHz. The attenuation edge decreased rapidly in magnitude as the angle θ between \mathbf{H} and the z axis was increased from zero, and disappeared entirely for $\theta \gtrsim 1^\circ$.

A second feature in the attenuation data was the existence of an attenuation peak, several hundred G wide, at $H_{c11} = 68.2 \pm 0.7$ kG. For \mathbf{H} exactly along the z axis this attenuation peak was masked by the attenuation edge described earlier. However, when the magnetic field made a small angle with the z axis, the attenuation edge was reduced in magnitude and the peak was easily observed. The height of the attenuation peak was greater than 5 dB/cm in the frequency range 10–60 MHz. Figure 3 shows a recorder tracing of the attenuation with \mathbf{H} near, but not exactly along, the z axis. Both the attenuation peak and the attenuation edge are clearly visible in this trace.

The dependence of the attenuation peak on the angle θ was studied at $77^\circ K$ with 30- and 50-MHz waves, and in the angular interval $0^\circ \leq \theta \leq 60^\circ$. As θ increased the attenuation peak became broader and the field H_c at the center of the peak increased. The rate of increase of H_c with θ was slow for small θ but became appreciable at large θ . At $\theta = 15^\circ$, H_c was about 8 kG above the value 68.2 kG for $\theta = 0$, whereas at $\theta = 24^\circ$, H_c was about 20 kG above the value for $\theta = 0$.

²³ S. Foner and Y. Shapira, Phys. Letters 29A, 276 (1969).

Experiments were also carried out at 4.2°K using 10- and 30-MHz waves. The results were similar to those obtained at 77°K, except that the attenuation peaks at finite θ were narrower.

Attenuation measurements at 77°K were performed also on the samples Elba-2 and Elba-3 with 30-MHz waves. The results in Elba-2 were qualitatively similar to those obtained in Brazil-1, except that the attenuation peak at $H_{c11} \cong 68$ kG was 3 kG wide. A small attenuation edge (~ 1 dB/cm) was observed in Elba-3 when \mathbf{H} was along the z axis.

4. $q \parallel x$ —Fast Shear Wave, $T = 77^\circ K$

For $q \parallel x$ there exist two pure nondegenerate shear modes. The directions of ion displacement ξ for these two modes do not coincide with the trigonal and bisectrix axes. The fast shear mode is discussed first.

Attenuation measurements were performed at 77°K using 24–60-MHz waves. With $\mathbf{H} \parallel z$, the attenuation increased abruptly at H_{c11} , and no acoustical echoes could be seen at $H > H_{c11}$. Lower limits for the magnitude of the attenuation edge are 10 dB/cm at 24 MHz and 8 dB/cm at 40 MHz. When θ was about 1° to 2°, the attenuation at $H > H_{c11}$ was: (a) smaller than in the case $\theta = 0$ so that acoustical echoes could be seen, and (b) was a monotonically decreasing function of H . Figure 4 compares the results for $\theta = 0$ and for $\theta \approx 1^\circ$. At $\theta \approx 4^\circ$ the attenuation increased abruptly at $H = H_{c11}$, but decreased rapidly with H at $H > H_{c11}$, resulting in an asymmetric attenuation peak with a maximum at $H = H_{c11}$.

A large change in the ultrasonic velocity was observed near H_{c11} at $\theta \approx 1^\circ$ – 2° . At these angles the attenuation at $H > H_{c11}$ was high but acoustical echoes could be seen. The video signal of the echo pattern for 24- and 40-MHz waves was observed on the oscilloscope. The time separation between successive echoes (measured from the maximum amplitude of one echo to the maximum amplitude of the next echo) was about 5% larger at $H > H_{c11}$ than at $H < H_{c11}$. It should be pointed out that the velocity obtained from this type of measurement does not always agree with the phase velocity.²⁰

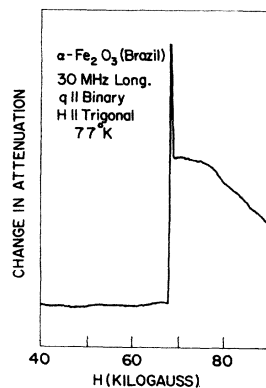


FIG. 3. Recorder tracing of the attenuation of a 30-MHz longitudinal wave with $q \parallel x$ and \mathbf{H} near, but not exactly along the z axis. The recorder response to the attenuation is nonlinear.

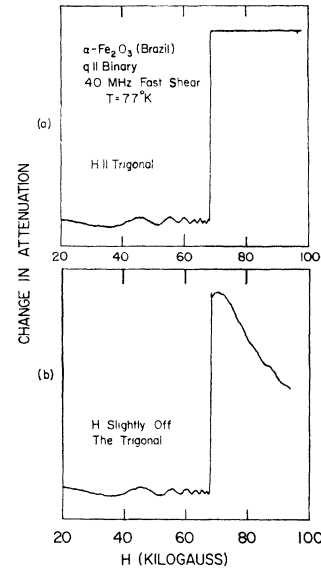


FIG. 4. Recorder tracing of the attenuation of a 40-MHz (fast) shear wave with $q \parallel x$ at 77°K. (a) $\mathbf{H} \parallel z$. (b) \mathbf{H} about 1° off the z axis. The recorder response to the attenuation is nonlinear. In (a), the flat portion of the curve at $H > H_{c11}$ corresponds to the absence of detectable echoes.

Experiments were also carried out at 77°K on the samples Elba-3 and 4 using 30- and 50-MHz waves. The results for $\mathbf{H} \parallel z$ were similar to those obtained in Brazil-1, except that the rise in the attenuation near the spin-flop transition took place over several kG instead of few hundred G.

5. $q \parallel x$ —Slow Shear Wave, $T = 77^\circ K$

The attenuation of 8.5–58-MHz waves was measured at 77°K in the angular range $0^\circ \leq \theta \lesssim 4^\circ$. The results were similar to those obtained for the fast shear mode with $q \parallel x$.

6. $q \parallel \xi \parallel y$ —Longitudinal Wave, $T = 77, 4.2^\circ K$

Attenuation results at 77°K with 10–50-MHz waves are similar to those obtained with longitudinal waves propagating along the x axis, and can be summarized as follows: (1) For $\mathbf{H} \parallel z$ the attenuation increases abruptly at H_{c11} and remains high at $H > H_{c11}$. (2) This attenuation edge decreases rapidly in magnitude as θ increases from zero, and disappears entirely at angles greater than 1°–2°. (3) A sharp attenuation peak occurs at H_{c11} . The full width at half-height of the peak is about 300 G and its magnitude is greater than 5 dB/cm at 30 MHz. The peak is not very sensitive to θ for $0^\circ \leq \theta \lesssim 3^\circ$.

Measurements of the phase velocity, at 77°K with 30-MHz waves and with \mathbf{H} near the z axis, showed that the velocity has a sharp minimum at H_{c11} and is fairly constant at $H > H_{c11}$. The velocity dip at H_{c11} was reproducible in all runs, and had a magnitude of $\sim 0.6\%$. On the other hand, the value of the velocity at $H > H_{c11}$

varied from run to run and was anywhere between the value at zero magnetic field and 0.5% below this value. This variation in the results at $H > H_{c11}$ may be related to the great sensitivity of the attenuation edge to the angle θ (often, an increase in attenuation is accompanied by a decrease in the velocity). Observing the video display of the echo pattern on the oscilloscope, no large ($\geq 1\%$) change in the time separation between echoes was detected near H_{c11} .

One experiment, performed at 4.2°K with \mathbf{H} near the z axis, showed a sharp attenuation peak at H_{c11} for a 50-MHz wave. The peak occurred 0.4 ± 0.4 kG above the value at 77°K, and the full width at half-height was ~ 200 G. A 0.6% dip in the phase velocity was also observed and is shown in Fig. 5.

Attenuation measurements on the sample Elba-3, at 77°K with a 30-MHz wave and with \mathbf{H} near the z axis, showed no observable effect near H_{c11} .

7. $q \parallel y, \xi \parallel x$ —Shear Wave, $T = 77, 4.2^\circ\text{K}$

Measurements at 77°K were performed using 7.5–60-MHz waves. With $\mathbf{H} \parallel z$, the attenuation increased abruptly at H_{c11} , and no acoustical echoes were observed at $H > H_{c11}$. A lower limit for the magnitude of the attenuation edge for 30- and 50-MHz waves is 7 dB/cm. At $\theta \approx 3^\circ$, the attenuation at $H > H_{c11}$, while higher than at $H < H_{c11}$, was sufficiently low for acoustical echoes to be observed. The attenuation in this case decreased with increasing H at $H > H_{c11}$.

The time separation between the maxima of successive acoustical echoes was measured with a 30-MHz wave at 77°K and with \mathbf{H} about 3° from the z axis. This time separation was about 5% larger at $H > H_{c11}$ than at $H < H_{c11}$. In the same run the phase velocity showed a sharp dip of about 0.7% at H_{c11} , but was only about 0.5% lower at $H > H_{c11}$ than at $H < H_{c11}$. Some distortion of the shape of the acoustical echoes occurred at $H > H_{c11}$. At $H < H_{c11}$ the shape of the video signal of each of echoes, as observed on the oscilloscope, was symmetric,

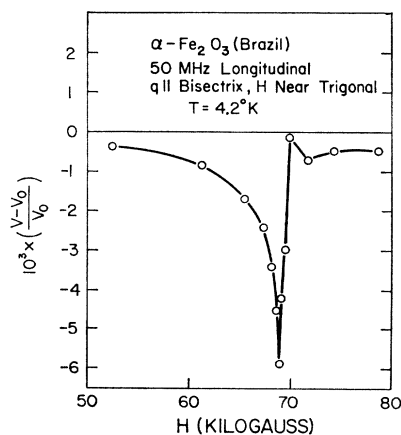


FIG. 5. Magnetic field variation of the phase velocity V of a 50-MHz longitudinal wave with $q \parallel y$ and \mathbf{H} near the z axis at 4.2°K.

whereas at $H > H_{c11}$ the echoes were asymmetric. Specifically, at $H > H_{c11}$ the amplitude of the rf signal of each echo rose in time more slowly than it fell off.

Attenuation measurements at 4.2°K were carried out at $\theta = 0$ and $\theta \approx 3^\circ$ using 30-MHz waves. The results were similar to those obtained at 77°K. The magnitude of the attenuation edge at H_{c11} was greater than 6 dB/cm.

Experiments on the samples Elba-3 and 4 were carried out at 77°K using 30- and 50-MHz waves and with $\mathbf{H} \parallel z$. The results were similar to those obtained in Brazil-1, except that the rise in attenuation near the spin-flop transition took place over several kG.

8. $q \parallel y, \xi \parallel z$ —Shear Wave, $T = 77^\circ\text{K}$

Attenuation and velocity measurements were performed at 77°K using 24–56-MHz waves and at angles $0^\circ \leq \theta \leq 3^\circ$. The results were similar to those obtained for the shear mode with $q \parallel y$ and $\xi \parallel x$. An attenuation edge near H_{c11} was also observed at 77°K in the samples Elba-3 and 4. The attenuation edge in these samples was much broader than in Brazil-1.

9. Temperature Variation of H_{c11}

To trace the temperature variation of H_{c11} , the attenuation of 30- and 50-MHz longitudinal waves propagating along the z axis was measured as a function of H at various temperatures. With $\mathbf{H} \parallel z$, a sharp peak in the attenuation (see Fig. 1) marked the position of H_{c11} . At temperatures $T \gtrsim 220^\circ\text{K}$, the magnitude of this absorption peak, for longitudinal waves propagating along the z axis, was very small, and H_{c11} could not be determined in this fashion. To determine H_{c11} in this temperature range, the attenuation of 30-MHz longitudinal waves with $q \parallel x$ was measured as a function of H . With $\mathbf{H} \parallel z$, a sharp attenuation edge marked the position of H_{c11} . The temperature variation of H_{c11} is shown in

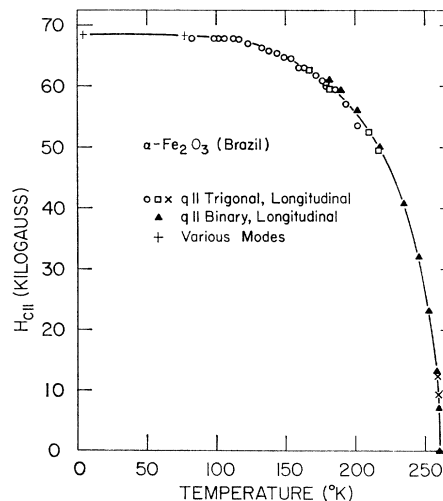


FIG. 6. Temperature variation of the spin-flop field $H_{c11}(\mathbf{H} \parallel z)$. Results obtained using different acoustical modes are represented by different symbols.

Fig. 6. The detailed variation of H_{c11} and H_{c11}^2 at temperatures close to T_M is shown in Fig. 7.

B. Field Normal to Trigonal Axis

Attenuation measurements were made with the magnetic field either along a bisectrix (y) direction, or along a binary (x) direction. The measurements were made at temperatures $77^\circ\text{K} < T < 300^\circ\text{K}$, and in magnetic fields up to 200 kG.

1. $\mathbf{H} \parallel y$

Measurements were made with longitudinal waves propagating either along that y direction which was parallel to \mathbf{H} , or along that x axis which was normal to \mathbf{H} (there are three binary and three bisectrix directions in the trigonal plane).

Figure 8 shows a trace of the ultrasonic attenuation of a 50-MHz longitudinal wave propagating along the x axis. A peak in the attenuation at 160.8 ± 2 kG is clearly visible. Subsequent differential magnetization

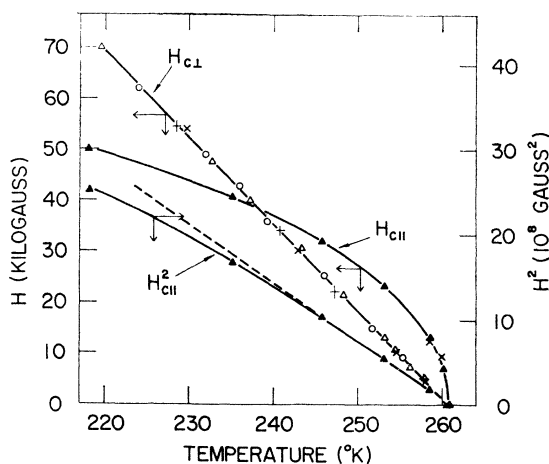


FIG. 7. Temperature variation of H_{c11} , H_{c11}^2 , and H_{c1} near T_M . The dashed line is a straight-line approximation to $H_{c11}^2(T)$ with $dH_{c11}^2/dT = -6.8 \times 10^7 \text{ G}^2/\text{°K}$.

measurements in pulsed fields performed by Foner²³ on the same sample showed that at this field value the magnetization changes abruptly (the derivative of the magnetization in respect to H exhibited a spike), indicating the existence of a first-order magnetic phase transition. We shall designate the field at this phase transition by H_{c1} . No other magnetic phase transition for $\mathbf{H} \parallel y$ was detected either ultrasonically or by differential magnetization measurements in pulsed fields.²⁴ The attenuation peak for 30- and 50-MHz longitudinal waves propagating along the x axis was observed at all temperatures from 77°K to T_M . The width at half-

²⁴ With \mathbf{H} along one of the bisectrix axes and at $T = 77^\circ\text{K}$, a small peak in the attenuation was observed at 92 kG. The temperature variation of this peak was studied at $T_M > T > 77^\circ\text{K}$. The small attenuation peak was not present, however, when \mathbf{H} was along a different bisectrix axis. A study of the angular dependence of this attenuation peak indicated that it originated from the (10 $\bar{1}$ 1) twin lamellae which were present in this sample (Sec. II).

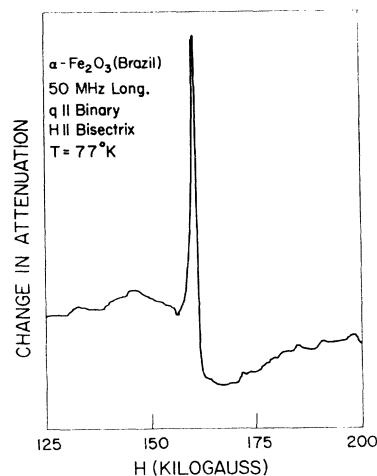


FIG. 8. Recorder tracing of the attenuation of a 50-MHz longitudinal wave with $q \parallel x$ and $\mathbf{H} \parallel y$ at 77°K . The recorder response to the attenuation is nonlinear.

height of this peak was 1–2 kG over the entire temperature range.

Measurements with 30-MHz longitudinal sound waves propagating along a y direction (parallel to \mathbf{H}) were performed at $160^\circ\text{K} < T < T_M$. A large attenuation peak at H_{c1} was observed at all temperatures. The width of the peak at half-height was 1–3 kG in all cases. The temperature variation of H_{c1} is shown in Fig. 9. The detailed variation of H_{c1} near T_M is shown in Fig. 7.

2. $\mathbf{H} \parallel x$

Measurements were made with 30-MHz longitudinal waves propagating either along that x direction which was parallel to \mathbf{H} or along that y direction which was normal to \mathbf{H} . The results for both modes of propagation were similar, and can be described as follows: At temperatures just below T_M the attenuation as a function of

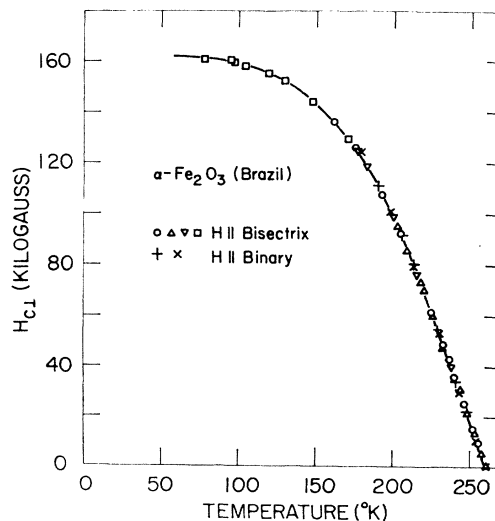


FIG. 9. Temperature variation of the transition field $H_{c1}(\mathbf{H} \perp z)$. Results for both $\mathbf{H} \parallel x$ and $\mathbf{H} \parallel y$ are included.

\mathbf{H} exhibited a sharp peak. As the temperature was lowered, the attenuation peak became asymmetric. In an increasing magnetic field, the attenuation rose slowly to its maximum value, and then dropped abruptly. The asymmetry in the line shape of the attenuation peak became more and more pronounced as the temperature was lowered. The field at the maximum of the attenuation peak was measured from 180°K to T_M and is shown in Fig. 9. As can be seen, this field agrees with the transition field obtained with \mathbf{H} along the y direction. The only difference between the results with $\mathbf{H}\parallel y$ and those with $\mathbf{H}\parallel x$ is that in the former case, the absorption peaks were narrow and more or less symmetric at all temperatures, while in the latter case, the peaks were broader and very asymmetric at low temperatures.

3. Observations near T_M

The temperature variation of the attenuation of 30-MHz longitudinal waves propagating along the x and y directions was measured between 240 and 300°K at $H=0$, and at low applied magnetic fields. As the temperature increased towards T_M , the attenuation at zero magnetic field rose abruptly, passed through a sharp maximum at T_M , and remained high at $T > T_M$. This behavior is shown in Fig. 10(a). The temperature at which the sharp peak in the attenuation occurred was $T_M = (260.6 \pm 0.5)^\circ\text{K}$, which we identify as the Morin transition. Flanders and Remeika²⁵ determined the

Morin transition of "pure" hematite to be $T_M \approx 262^\circ\text{K}$, with a variation of several degrees between samples grown from different melts. Besser *et al.*¹⁰ quote $T_M = 263^\circ\text{K}$ for pure hematite. The data which are presented in both of these references indicate that T_M is sensitive to impurities (especially to Ti). However, no appreciable effect on T_M due to the impurities in the sample Brazil-1 is expected because of their low concentrations.

When a magnetic field of several hundred G was applied in the xy plane, the attenuation at $T > T_M$ was reduced to its value at $T < T_M$, but the attenuation peak near T_M remained. This is shown in Fig. 10(b). The width at half-height of the attenuation peak in this figure is $\sim 0.4^\circ\text{K}$. A magnetic field of several hundred G applied in the xy plane had no appreciable effect on the attenuation at $T < T_M$. The present results for the temperature variation of the attenuation near T_M are similar to the results of internal friction measurements by Makkay *et al.*¹⁶ at frequencies of 125 and 150 kHz.

IV. DISCUSSION

The discussion below is divided into two parts. In Sec. IV A, physical mechanisms which may be responsible for the ultrasonic behavior near the magnetic phase transitions of hematite are discussed. Section IV B is devoted to the temperature dependence of H_{c11} and H_{c1} .

A. Ultrasonic Behavior near Magnetic Phase Transitions

The salient features of the ultrasonic behavior near the magnetic phase transitions of hematite can be summarized as follows:

(1) At zero magnetic field, the attenuation of longitudinal waves propagating in the trigonal (xy) plane is larger at $T > T_M$ than at $T < T_M$. A magnetic field of a few hundred G applied in the xy plane reduces the attenuation at $T > T_M$ to its value at $T < T_M$.

(2) At zero field, the attenuation of longitudinal waves propagating in the xy plane, as a function of T , exhibits a sharp peak at T_M . This peak is not removed by a magnetic field of several hundred G applied in the xy plane.

(3) At $T < T_M$ and with $\mathbf{H}\parallel z$, the attenuation at $H > H_{c11}$ is higher than at $H < H_{c11}$. This is true for all the acoustical modes which were investigated except for the longitudinal mode with $\mathbf{q}\parallel z$. The excess attenuation at $H > H_{c11}$ is reduced rapidly when the magnetic field is tilted away from the z axis. For some modes, the attenuation at $H > H_{c11}$ is accompanied by an appreciable change in the sound velocity.

(4) At $T < T_M$ and with the field applied along the trigonal axis, the attenuation of all the longitudinal modes exhibits a sharp peak at H_{c11} . For the shear modes, the large increase in attenuation at H_{c11} (i.e., the attenuation edge) makes it difficult to ascertain whether

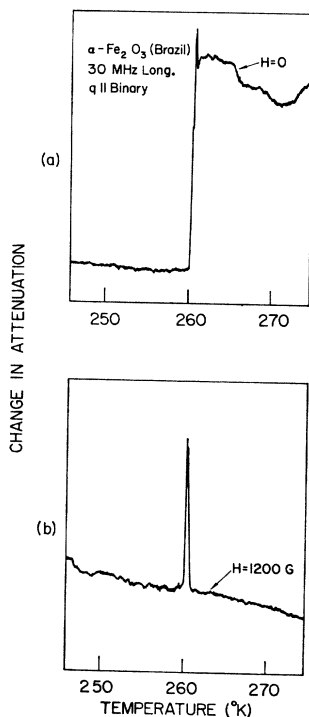


FIG. 10. Recorder tracing of the attenuation of a 30-MHz longitudinal wave with $\mathbf{q}\parallel x$. (a) $H=0$. (b) With a field $H=1200$ G applied along the x axis.

²⁵ P. J. Flanders and J. P. Remeika, *Phil. Mag.* **114**, 1271 (1965).

a sharp attenuation peak exists at H_{c11} . The attenuation peak at H_{c11} for the longitudinal modes does not disappear as \mathbf{H} is rotated away from the z axis by several degrees.

(5) At $T < T_M$ and with \mathbf{H} normal to the trigonal axis, the attenuation of longitudinal waves propagating in the trigonal plane exhibits a peak at H_{c1} .

1. Domain-Wall Motion

A qualitative explanation of these observations may be given in terms of domains.²⁶ An antiferromagnetic sample, like a ferromagnetic sample, may consist of several domains separated from each other by domain walls. In each domain the orientation of the spins for each of the antiferromagnetic sublattices is fixed. However, the orientation of the spins varies in general from one domain to another. Because of the magnetoelastic coupling, an applied elastic stress may prefer one orientation of the spins over another. In that case, domains with spin orientations close to the preferred orientation should grow at the expense of domains with unfavorable spin orientations. The changes in the sizes of the domains are accomplished by displacements of domain walls. When a sound wave propagates through an antiferromagnet, the alternating elastic stress associated with the sound wave may lead to a periodic motion of the domain walls. Assuming that there are frictional forces which tend to damp the domain-wall motion, one expects that the sound wave will lose energy in driving in the domain walls. Ultrasonic attenuation due to domain-wall motion in ferromagnets is well known.²⁷ That a similar attenuation mechanism exists in antiferromagnets was suggested by several workers.²⁸ In particular, Makkay *et al.*¹⁶ have interpreted some of their internal friction results in hematite in terms of energy losses due to domain-wall motion. As shown below, this loss mechanism may also account for the present results.

Sound absorption due to domain-wall motion can take place only if the elastic stress associated with the sound wave modifies the free energy of different domains by different amounts, thereby preferring the growth of one domain at the expense of another. For certain domain configurations, however, any elastic stress changes the free energy of all the domains by the same amount. In ferromagnets, for example, an elastic stress does not lead to a displacement of a wall between domains whose magnetization directions differ by 180° .²⁷ In uniaxial antiferromagnets of the easy-axis type (e.g., MnF_2) the only domains which can exist at zero magnetic field are such that the orientations of the spins in one domain can

be obtained from the orientations in an adjacent domain by interchanging the two antiferromagnetic sublattices, i.e. if in one domain the spins of sublattice A point up and those in sublattice B point down, then in an adjacent domain, the A spins are down and the B spins are up. An elastic stress should change the free energies of such domains by the same amount. Hence, ultrasonic absorption due to domain-wall motion is not expected in this case.

Turning to hematite, we know that at $T > T_M$ and $H = 0$ the spins are in the trigonal (xy) plane. Because the z axis is a threefold axis, to any orientation of the spins in the xy plane, there correspond other orientations, related to it by symmetry, which have the same free energy. Thus, no single spin orientation is preferred over all other orientations. Actually, the anisotropy in the xy plane of an ideal sample of hematite is very small²⁹ so that all directions in that plane are practically degenerate. The fact that there does not exist a unique orientation for the spins in the xy plane leads to the possibility of domains with spins oriented along different directions. These orientations, all normal to the z axis, are represented schematically in Fig. 11 by N_1 , N_2 , and N_3 (there may be more than three orientations in a real sample). Domains in hematite at $T > T_M$ were observed by the powder technique,³⁰ by the Faraday effect,³¹ and by the electron-shadow-pattern method.³² The domains had typical linear dimensions of order 0.1 mm. Eaton *et al.*³⁰ observed that the domain walls in a synthetic single crystal of hematite disappeared when a magnetic field $H > 25$ G was applied in the xy plane. Such a field prefers one orientation of the spins over all other orientations. The work of Flanders and Remeika²⁵ indicates that the magnitude of the field in the xy plane, necessary to obtain a single domain, varies from about 1 G to several hundred gauss, depending on the sample.

At $T < T_M$ and $H = 0$, the spins in hematite are

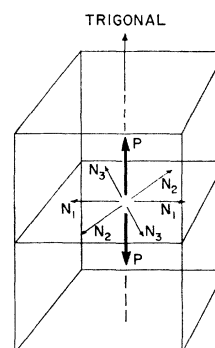


FIG. 11. Schematic representation of spin configurations in hematite. N_1 , N_2 , and N_3 represent configurations with spins normal to the z axis. P represents a configuration with spins parallel to the z axis.

²⁶ For a review of domains in antiferromagnets see M. M. Farztdinov, *Usp. Fiz. Nauk* **84**, 611 (1964) [English transl.: *Soviet Phys.—Usp.* **7**, 855 (1965)].

²⁷ W. P. Mason, *Physical Acoustics and the Properties of Solids* (D. Van Nostrand, Inc., Princeton, N. J., 1958), Chap. 8.

²⁸ See, for example, R. Street and B. Lewis, *Phil. Mag.* **1**, 663 (1956).

²⁹ A. Tasaki and S. Iida, *J. Phys. Soc. Japan* **18**, 1148 (1963).

³⁰ M. Blackman and B. Gustard, *Nature* **193**, 360 (1962); J. A. Eaton, A. H. Morrish, and C. W. Searle, *Phys. Letters* **26A**, 520 (1968).

³¹ H. J. Williams, R. C. Sherwood, and J. P. Remeika, *J. Appl. Phys.* **29**, 1772 (1958).

³² M. Blackman, G. Haigh, and N. D. Lisgarten, *Proc. Roy. Soc. (London)* **A251**, 117 (1959); G. Kaye, *ibid.* **78**, 869 (1961).

generally believed to be oriented parallel to the z axis.³³ This spin configuration is shown in Fig. 11 as P . The only type of domains which can exist in this case is the type discussed earlier for the case of a uniaxial antiferromagnet with an easy axis. Such a domain configuration is not expected to lead to ultrasonic attenuation by domain-wall motion. The same is true at $T < T_M$ when a magnetic field $H < H_{c11}$ is applied along the z axis. However, if \mathbf{H} is exactly along the z axis and $H > H_{c11}$, then a domain configuration similar to the one at $T > T_M$ and $H = 0$ is expected. If $H > H_{c11}$, but the field makes an angle $\theta \gtrsim 1^\circ$ with the z axis, then the component of the field in the xy plane will cause the sample to become a single domain.

Consider the temperature dependence of the attenuation of longitudinal waves propagating in the xy plane at $H = 0$. For temperatures $T < T_M$, attenuation due to domain-wall motion is not expected. At $T > T_M$, on the other hand, the elastic stress associated with the sound wave should not change the free energies of the domains N_1 , N_2 , and N_3 in Fig. 11 equally, because the uniaxial stress associated with the longitudinal wave cannot make the same angle with the spins in all three domains. It follows that attenuation due to domain-wall motion should exist at $T > T_M$. This may explain why the attenuation at $T > T_M$ is higher than at $T < T_M$. The decrease in attenuation which results from the application of a magnetic field in the xy plane at $T > T_M$ is also explained by the domain picture. Such a field transforms the entire sample into a single domain, thus removing the loss mechanism.

Consider Fig. 11. At T_M , the spin orientation, in zero field, changes from orientation P to orientations N_1 , N_2 , N_3 . One then expects that in a narrow temperature interval near T_M both orientation P and one or more of the orientations N_1 , N_2 , N_3 coexist. In this temperature interval there will then be two groups of domains. One group consists of domains with orientation P , and the second group with orientations N_1 , N_2 and N_3 . Such a domain configuration has, in fact, been observed.³¹ An elastic stress will, in general, favor or disfavor orientation P relative to the N orientations. Thus, near T_M , the motion of walls between P domains and N domains (in addition to walls between different N domains) may lead to ultrasonic attenuation. This may be the origin of the attenuation peak at T_M . A weak magnetic field ($H \sim 1$ kG) applied in the xy plane creates a preferred direction for the spins in that plane, and also shifts the transition temperature slightly. However, even in the presence of such a field there should exist, near the transition, domains where the spins are nearly along the z direction and domains with spins along the preferred direction in the xy plane. Because of the motion of the

walls separating these two types of domains, the attenuation peak near T_M should not disappear in a weak magnetic field, in agreement with observation.

The spin-flop transition at $H_{c11}(T < T_M, \mathbf{H} \parallel z)$ is similar to the Morin transition in zero field. In both cases the spin orientation changes from a direction parallel to the z axis to a direction normal to it. Using the same arguments as those used for the attenuation near T_M , one expects that: (1) the attenuation at $H > H_{c11}$, with \mathbf{H} exactly along the z axis, will be higher than at $H < H_{c11}$, (2) that this excess attenuation should disappear as \mathbf{H} is tilted away from the z -axis, and (3) that an attenuation peak will occur at H_{c11} . An exception to (1) is the case of a longitudinal wave propagating along the z axis. The elastic stress associated with this wave changes the free energy of all the N domains (Fig. 11) by the same amount so that attenuation due to domain-wall motion is not expected in this case. All these conclusions are in agreement with experiment. (See Figs. 1–4.)

Turning to the transition at $H_{c1}(T < T_M, \mathbf{H} \perp z)$, the experiments of Flanders¹⁵ indicate that, at least for T not too far below T_M , an abrupt change in the magnetization occurs at H_{c1} . The results of Foner²³ show that also at 77°K an abrupt change in the magnetization occurs at H_{c1} . It therefore appears that at $77^\circ\text{K} < T < T_M$, the orientation of the spins changes in a discontinuous fashion at H_{c1} . One then expects that domains with different spin orientations will coexist at H_{c1} . This may explain the attenuation peak observed at this transition. One puzzling feature is the difference between the line shape of the attenuation peak for $\mathbf{H} \parallel x$ and the one for $\mathbf{H} \parallel y$ at low temperatures.

The foregoing arguments indicate that the ultrasonic data can be explained qualitatively in terms of stress-induced motion of domain walls. The magnitude of the attenuation due to this mechanism should depend on the domain configuration and the relaxation time for domain-wall motion. Since these factors are expected to vary from sample to sample, the magnitude of the attenuation should differ from one sample to another, in agreement with observation. It is also clear that a calculation of the attenuation in a particular sample cannot be made unless the domain configuration and the relaxation time for domain-wall motion are known.

2. Spin Waves

The preceding discussion concentrated on the possibility of ultrasonic attenuation due to domain-wall motion. Other attenuation mechanisms which can occur inside a single domain should, however, also be considered. We therefore discuss briefly the possibility of sound attenuation due to spin waves.³⁴

In general, an rf sound wave may interact with low-frequency magnons in an antiferromagnet. The simplest

³³ There is, however, some evidence [A. H. Morrish *et al.*, Phys. Letters 7, 177 (1963)] that at $T < T_M$ and $H = 0$, the spins are not exactly along the trigonal axis. If this turns out to be the case, the possible existence of domain configurations other than those described here will have to be considered.

³⁴ Literature on ultrasonic attenuation due to spin waves in antiferromagnets is cited in Ref. 2.

of such interactions is the phonon-magnon resonance which can occur when the wave vectors and frequencies of the sound and spin waves coincide (actually, absorption due to phonon-magnon resonance may occur even if the frequencies of the two waves do not exactly coincide, provided that these frequencies do not differ by more than the linewidth of the resonance). If, in the magnon spectrum there exists an energy gap which is sufficiently large so that the frequencies of the magnon and phonon differ appreciably from each other, then phonon-magnon resonance is not possible. Attenuation of sound may also result from more complicated processes which involve more than one magnon. If magnons exist with energies which are not high compared to kT , then the number of these magnons at thermal equilibrium may be appreciable, and multimagnon processes may become effective. Such processes should become less effective if in the magnon spectrum there exists a gap which is large compared to kT . The attenuation due to multimagnon processes should depend on temperature.

Low-frequency spin waves may exist in an antiferromagnet if the energy required to change the orientation of the spins is small. In hematite, at $T > T_M$ and $H = 0$, the spins lie in the xy plane. Since the anisotropy energy in this plane is very small, low-energy magnons are expected. These low-energy magnons were investigated both theoretically and experimentally.³⁵ The energy gap for this spin-wave spectrum, measured in units of magnetic field, is about 4 kG. The gap is not greatly affected by an external magnetic field of several hundred gauss applied in the xy plane.

There are several arguments which suggest that the observed ultrasonic attenuation at $T > T_M$ and $H = 0$ is not due to these low-frequency spin waves. Phonon-magnon resonance is unlikely because the energy gap is ~ 4 kG, whereas observed magnon linewidths are about several hundred gauss. In addition, had the magnon linewidth in our sample been large enough to permit resonance absorption of sound waves at $H = 0$, it should have also allowed resonance absorption when a field of several hundred gauss was applied in the xy plane, since such a field hardly affects the magnon energy gap. The last conclusion disagrees with observation. There is also no obvious reason why multimagnon processes should be strongly affected by a field of several hundred gauss applied in the xy plane.

At $T < T_M$ and for $\mathbf{H} \parallel z$, a spin mode exists at $H > H_{c11}$ which is similar to the low-frequency spin mode which exists at $T > T_M$ and $H = 0$. Arguments similar to those just given indicate that it is unlikely that the observed large attenuation of many acoustical modes at $H > H_{c11}$ is due to these spin waves.

For a simple uniaxial antiferromagnet of the easy-axis type in a field directed along this axis, the frequency of one of the two usual antiferromagnetic spin modes goes

³⁵ P. Pincus, Phys. Rev. Letters **5**, 13 (1960); S. J. Williamson and S. Foner, Phys. Rev. **136**, A1102 (1964). See also Ref. 29.

essentially to zero at the spin-flop transition. Phonon interactions with this spin mode may then occur.³⁴ It is possible that also in hematite, such a low-frequency spin mode exists near the phase transitions at $H_{c11}(T < T_M)$ and at $T_M(H = 0)$. Such a low frequency mode may then be responsible for the attenuation peaks observed near these magnetic phase transitions. It should be mentioned, however, that attempts to observe low-frequency spin waves near H_{c11} and near the Morin transition by resonance absorption of low-frequency microwaves were not successful, and that there are experimental data which indicate that at these transitions there still remains a substantial gap in the spin-wave spectrum.^{23,36} Thus, the existence of low-frequency magnons near $H_{c11}(T < T_M)$ and near T_M (at $H = 0$) is doubtful.

In summary, the explanation of the observed ultrasonic phenomena in terms of domain-wall motion appears to be more satisfactory than the explanation in terms of interactions with spin waves.

B. Temperature Variation of H_{c11} and H_{c1}

The temperature variation of H_{c11} and H_{c1} is shown in Figs. 6 and 9. The detailed variation of these fields near T_M is shown in Fig. 7. These data will now be discussed.

The magnetic phase transition at H_{c11} is known to be a first-order transition which is accompanied by an abrupt change in the magnetization. Our values for the transition fields at 77 and 4.2°K are $H_{c11} = 68.2 \pm 0.7$ kG, and $H_{c11} = 68.6 \pm 0.8$ kG, respectively. The value at 77°K agrees with the results of magnetization measurements on the same sample,²³ and also compares favorably with earlier results on natural⁷⁻⁹ and synthetic¹⁰⁻¹² hematite single crystals, which gave values for H_{c11} ranging from about 63 to about 68 kG. In the intermediate temperature range $180^\circ\text{K} \lesssim T \lesssim 240^\circ\text{K}$, our experimental points lie somewhat lower than those of Besser *et al.*,¹⁰ somewhat higher than those of Kaneko and Abe,⁹ and in fair agreement with those of Foner⁷ and of Voskanyan *et al.*¹² As can be seen from Figs. 6 and 7, the derivative $-dH_{c11}/dT$ becomes large as T approaches T_M . On the other hand, a plot of H_{c11}^2 versus T at temperatures near T_M gives approximately a straight line (see Fig. 7). At $T = T_M$ we have $dH_{c11}^2/dT = -(6.8 \pm 0.3) \times 10^7$ G²/°K. The results near T_M are in good agreement with those obtained by Flanders *et al.*¹⁴

It is possible to get an insight into the temperature variation of H_{c11}^2 near T_M by considering a simple model in which only the first-order single-ion anisotropy (of the form $K_1 \cos^2 \varphi$, where φ is the angle between the spin direction and the z axis) is taken into account.³⁷ Ac-

³⁶ S. Foner and S. J. Williamson, J. Appl. Phys. **36**, 1154 (1965); S. V. Mironov, V. I. Ozhogin, E. G. Rudashevskii, and V. G. Shapiro, Zh. Eksperim. i Teor. Fiz. Pis'ma v Redaktsiyu **7**, 419 (1968) [English transl.: Soviet Phys.—JETP Letters **7**, 329 (1968)].

³⁷ G. Cinader and S. Shtrikman, Solid State Commun. **4**, 459 (1966). See also Ref. 11.

ording to this model, H_{c11} is given by

$$H_{c11}^2 = 2H_E H_A - H_d^2, \quad (1)$$

where H_E is the exchange field, H_A is the anisotropy field, and H_d is the Dzyaloshinsky-Moriya field. The temperature variation of H_{c11} near T_M is determined essentially by the dependence of H_A on T . Since H_A varies smoothly with T near T_M ,³⁸ one can expand it about T_M in a Taylor series. At temperatures only slightly below T_M , one can neglect quadratic terms in $(T_M - T)$ and higher. Keeping in mind that $H_{c11} = 0$ at T_M , one then obtains

$$H_{c11}^2(T) = 2H_E(T - T_M)(dH_A/dT)_{T_M}, \quad (2)$$

which explains why H_{c11}^2 varies linearly with T at temperatures just below T_M .

As a quantitative check of this explanation, we calculate the slope dH_{c11}^2/dT using Eq. (2). From Fig. 8 of Ref. 38 we estimate $dH_A/dT \cong -2.6$ G/°K at $T = T_M$. The exchange field H_E near T_M is expected to be approximately equal to H_E at 0°K, because $T_M \ll T_N$. The latter value can be calculated from Eq. (1) using the measured value $H_{c11} = 68.6$ kG and^{29,38} $H_A \cong 220$ G, $H_d \cong 24$ kG, giving $H_E \cong 1.2 \times 10^7$ G. This value is in reasonable agreement with the values 1.14×10^7 and 9.2×10^6 G for the exchange field near room temperature, as determined by Tasaki and Iida²⁹ from resonance and susceptibility measurements, respectively. Using $H_E = 1.2 \times 10^7$ G one obtains from Eq. (2) $dH_{c11}^2/dT \cong -6.2 \times 10^7$ G²/°K, in good agreement with the experimental value. Thus the simple model of Cinader and Shtrikman³⁷ accounts for the temperature dependence of H_{c11} . It should be stated, however, that this model does not account for the nature of the transition at H_{c1} .

From Figs. 7 and 9, we see that in the temperature interval $220^\circ\text{K} < T < T_M$, the transition field H_{c1} is proportional to $(T_M - T)$ with $dH_{c1}/dT = -(1.69 \pm 0.07)$ kG/°K. Flanders¹⁵ has recently measured H_{c1} in synthetic hematite at temperatures near T_M . He found $H_{c1} \propto (T_M - T)$ with $dH_{c1}/dT = -1.6$ kG/°K. Kaczér and Shalnikova¹³ obtained $dH_{c1}/dT = -1.5$ kG/°K at T_M . It should be noted that H_{c1} is approximately proportional to $(T_M - T)$ over a larger temperature interval than the one in which H_{c11}^2 is approximately proportional to $(T_M - T)$. Thus, the proportionality between H_{c11}^2 and H_{c1} observed by Flanders *et al.*¹⁴ near T_M is not maintained at temperatures far below T_M . At 77°K our data give $H_{c1} = 160.8 \pm 2$ kG, which agrees with magnetization measurements on the same sample,²³ but which is about 20% higher than the value obtained by Ozhogin and Shapiro,¹¹ and about 15% higher than the value extrapolated from the data of Voskanyan *et al.*¹² The origin of this discrepancy is not clear. It is

³⁸ J. O. Artman, J. C. Murphy, and S. Foner, Phys. Rev. 138, A912 (1965).

unlikely that the impurities in the sample Brazil-1, whose concentrations are very low, had any appreciable effect on H_{c1} . [Note added in proof. Recently Beyerlein and Jacobs reported the value $H_{c1} = 162 \pm 8$ kG at 77°K for a synthetic crystal of hematite. [Bull. Am. Phys. Soc. 14, 349 (1969)]]].

The nature of the transition at H_{c1} has been the subject of several recent studies. Using a model in which only the first order single-ion anisotropy is taken into account, Cinader and Shtrikman³⁷ concluded that the transition at H_{c1} takes place without a discontinuous change in the magnetization. Experiments by Flanders *et al.*^{14,15} have shown, however, that close to T_M there is a rapid change in the magnetization near H_{c1} . To explain their results these workers suggested that a second-order single-ion anisotropy (of the form $K_2 \cos^4 \varphi$) should be included in the free energy. More recently, Levitin and Shchurov³⁹ have studied the effect of the second order anisotropy on the transition at H_{c1} . They concluded that at $T > 200^\circ\text{K}$, the transition is of first order (discontinuous change in the magnetization), whereas at lower temperatures the character of the transition could not be ascertained. The magnetization data of Foner²³ indicate that the transition is still of first order at 77°K. The fact that the transition at H_{c1} is of first order was assumed in the explanation of the ultrasonic absorption peak at H_{c1} in terms of domain-wall motion.

Note added in proof. The entropy change ΔS at the Morin transition can be deduced from the magnetic analog of Clapeyron's equation, which can be written in this case as

$$\Delta S = -\sigma(dH_{c1}/dT)_{T_M}, \quad (3)$$

where σ is the weak ferromagnetic moment (in a single domain) at $T > T_M$. Letting²⁵ $\sigma \approx 0.4$ emu/g, we obtain $\Delta S \approx 0.68 \times 10^3$ erg/deg g or $\Delta S = 3.6 \times 10^3$ erg/deg cm³. From a study of the transition with $\mathbf{H} \parallel z$, Kaneko and Abe⁹ obtained $\Delta S = 0.6 \times 10^3$ erg/deg g, in good agreement with our value.

ACKNOWLEDGMENTS

The author is indebted to Professor D. R. Wones and Professor C. Frondel for kindly providing him with samples, to S. Foner for performing magnetization measurements on one of the samples and for many helpful comments, to P. J. Flanders for informative discussions, to A. N. Mariano for information on twins in hematite, to L. G. Rubin for advice on experimental techniques, and to E. J. Alexander and V. Diorio for technical assistance.

³⁹ R. Z. Levitin and V. A. Shchurov, Zh. Eksperim. i Teor. Fiz. Pis'ma v Redaktsiyu 7, 142 (1968) [English transl.: Soviet Phys.—JETP Letters 7, 110 (1968)].